Capillarity

Vol. 16, No. 2, p. 27-38, 2025

Original article

Experimental study of carbonated water imbibition in deep coal rocks using nuclear magnetic resonance spectroscopy

Liu Yang[1], Zhen Liu[1], Ziheng Zhao[1]*, Wenhong Li[2], Jiping Ding[3], Linghui Sun[4]

[1]State Key Laboratory for Tunnel Engineering, China University of Mining & Technology, Beijing 100083, P. R. China

[2]China National Petroleum Corporation U.S.A. Branch, Beijing 102200, P. R. China

[3]China Petroleum Engineering Technology Research and Development Co., Beijing 10053, P. R. China

[4]China Academy of Petroleum Exploration and Development, Beijing 100083, P. R. China

Keywords:
Coal rock
imbibition
carbonated water imbibition
nuclear magnetic resonance
pore structure

Cited as:
Yang, L., Liu, Z., Zhao, Z., Li, W., Ding, J., Sun, L. Experimental study of carbonated water imbibition in deep coal rocks using nuclear magnetic resonance spectroscopy. Capillarity, 2025, 16(2): 27-38.
https://doi.org/10.46690/capi.2025.08.01

Abstract:
The deep eastern edge of the Ordos Basin is rich in coalbed methane, presenting great potential for development. Meanwhile, CO_2 imbibition is an important method to increase production. To study the CO_2-water-rock interactions and microstructural damage characteristics before and after supercritical carbon dioxide immersion in deep coal rocks, CO_2 imbibition experiments were conducted on these rocks by using nuclear magnetic resonance and scanning electron microscopy imaging techniques. The results showed that CO_2 imbibition leads to pore dilatation and reveals the key role of coal rock anisotropy on imbibition efficiency under different physicochemical conditions. Specifically, the immersion of CO_2 produces cracks due to the brittle action of the coal rock, as well as calcite dissolution that exacerbates crack production and expansion. Due to adsorption of CO_2, part of the coal rock becomes swollen, which leads to detachment and changed the physical properties and surface characteristics of the coal rock.

1. Introduction

The eastern margin of the Ordos Basin in China is rich in coal rock gas resources. Currently, these are estimated at about 600 billion cubic meters, and the potential reserves are huge (Yuan, 2016; Bakhshian and Sahimi, 2017; Zhang et al., 2018; Yang et al., 2025a). However, high temperature, high pressure and the complex geological environment where deep coal rocks occur lead to their extremely low permeability. The severely restricted efficiency of coal rock gas exploration has become one of the main bottlenecks for the safe and efficient extraction of deep coal rock gas. Spontaneous imbibition is a process in which a wet-phase fluid displaces a non-wet-phase fluid by capillary force in complex porous media (Yang et al., 2025b). Composed of a capillary network system, the gas in the coal body is a non-wet phase fluid, while the water is a wet phase fluid, resulting in the spontaneous imbibition effect. Compared with conventional coal rock water injection, CO_2 imbibition will cause dissolution, leading to pore structure expansion, which prompts measures to prevent coal and gas outburst (Li et al., 2021; Xu et al., 2022). However, the change mechanism of reservoir pore structure after CO_2 immersion is still unclear and the flow law of carbonated water imbibition is complicated, making such prevention measures difficult to apply at present. Therefore, it is imperative to determine the influence of CO_2-water-rock interaction on the pore structure and imbibition capacity of coal rock, as well as the change characteristics of coal rock minerals before and after Super-

Yandy Scientific Press

*Corresponding author.
E-mail address: shidayangliu@cumtb.edu.cn (L. Yang); 13103859157@163.com (Z. Liu); 17731183524@163.com (Z. Zhao); g15666329379@163.com (W. Li); yzh1561650216@outlook.com (J. Ding); chen20230620@163.com (L. Sun).

Received April 21, 2025; revised May 18, 2025; accepted June 10, 2025; available online June 14, 2025.

critical CO_2 (SC-CO_2) treatment.

The process of CO_2 imbibition is affected by many factors, mainly including temperature, pressure, solution concentration, regeneration of the solution, activator content in the solution, circulation amount of solution, and other factors affecting system balance (Liu et al., 2021; Hou et al., 2022). The coal body is a complex porous medium. The imbibition process of water in the coal body can promote the desorption of gas, reducing the gas content in the coal seam and improving the gas drainage effect. The research results show that water imbibition and suction is the mechanism of oil displacement in fractured reservoirs (Huang et al., 2017), for which capillary force provides the main driving force (Yue et al., 2017; Yang et al., 2024). However, regarding the permeation and absorption effect, the migration process and distribution law of water in the coal body have rarely been studied. In response to this issue, some scholars have utilized microfluidic experiments and numerical simulations to study the characteristics of coal rock gas imbibition. Wang et al. (2017) constructed a mathematical model of dynamic imbibition based on the imbibition theory. Nguyen et al. (2018) conducted a microfluidic experimental study to quantitatively analyze the effect of fractures on recovery. Wei et al. (2024) conducted a series of online nuclear magnetic resonance analyses under different aspiration systems. Li et al. (2022b) quantified the influence of fracturing fluid and studied the nature of formation damage caused by fracturing fluid.

Numerous scholars have explored the spontaneous imbibition characteristics of coal rock through physical experiments. The spontaneous imbibition process mainly includes the displacement of adsorbed gas and wetting pores (Huang et al., 2020; Li et al., 2020). Recently, the physical experiments and testing methods for coal rock gas imbibition have become increasingly diversified. Especially, these include non-destructive monitoring methods such as Computed Tomography, supersonic wave, and Nuclear Magnetic Resonance (NMR) (Zhang et al., 2019; Li et al., 2022a, 2023; Fang et al., 2023). NMR is a particularly prominent method for the realistic and quantitative assessment of micro-production characteristics and multiphase flows within different cores. Lu et al. (2022) combined X-ray, Micro Computed Tomography and Scanning Electron Microscopy (SEM) to study the effects of pore fracture and mineral content on spontaneous imbibition, and found the insertion stone content to be positively correlated with the cumulative water content during spontaneous imbibition. Ma et al. (2022) studied the influence of different confining pressures on the spontaneous imbibition of water in coal, but no migration of water along the axis was observed in sandstone samples with different layering orientations. Wei et al. (2025) quantified the contribution of shale pores of different scales to suction recovery under different injection medium conditions.

Regarding the development of Coal Bed Methane (CBM), it has been found that calcite veins may have a significant impact. Xia et al. (2021) studied the factors influencing the infiltration and absorption of tight sandstone through petrophysical properties and fractal parameters. Therefore, it is necessary to investigate the influence of calcite veins on the mechanical properties of coal rock, as well as the softening rule of CO_2 on coal rock containing calcite veins. CO_2 imbibition causes coal rocks to expand. During the transformation process, the failure mode of high-order coal changes from brittle failure to ductile damage (Wei et al., 2019; Liao et al., 2021; Si et al., 2021). After CO_2 has been injected into the coal seam, some of the organic groups in coal are extracted, which can cause the coal matrix to shrink and expand (Cai et al., 2014; Chen et al., 2021; Niu et al., 2021; Liu et al., 2022). Cai (2021) explored the core issues and guiding principles underlying spontaneous imbibition in porous media, offering some valuable theoretical perspectives. Jiao et al. (2025) evaluated the content and microscopic distribution behavior of pore water through centrifugal-nuclear magnetic resonance experiments and theoretical models.

In summary, various scholars have carried out extensive research in the field of SC-CO_2 on the deterioration of the mechanical strength of coal rocks. Nevertheless, there are relatively few experimental studies on CO_2 imbibition and the physics before and after SC-CO_2 immersion. In addition, few scholars have addressed the softening pattern of coal rocks containing calcite veins under SC-CO_2 conditions. In this paper, we conduct CO_2 imbibition and SC-CO_2 immersion experiments on deep coal rock samples from the eastern margin of the Ordos Basin. Combined with SEM and NMR, we analyze the evolution of tight and loose coal rocks under different conditions during the imbibition process. The results provide important theoretical guidance and technical support for guiding carbonated water imbibition and SC-CO_2 immersion damage in deep coal rocks.

2. Samples and experimental methods

2.1 Samples

The No. 8 coal seam of the Benxi Formation of the Carboniferous System in the eastern margin of the Ordos Basin is rich in CBM resources, hence it has become a key exploration target for CBM development in recent years. Here, the spatial distribution of coal seams is stable and dominated by calcite veins. No. 8 coal seam is mainly bright coal and semi-dark coal with medium metamorphism. In this article, a sample of No. 8 coal seam was collected from a core well depth of 1,600-2,400 m.

CO_2 imbibition experiments were conducted to study CO_2-water-rock interactions. In addition, the mechanism of CO_2-induced pore damage was revealed using NMR techniques. Core plugs measuring 25 mm in diameter and 50 mm in length were prepared from three tight coal rocks and three loose coal rocks. The cut coal samples were subjected to spontaneous imbibition, forced imbibition and carbonated water imbibition. Fig. 1 presents schematic diagrams of the experimental samples and techniques.

2.2 Methods

2.2.1 Carbon dioxide imbibition

The T_2 and T_1-T_2 relaxation time spectra were monitored and obtained by an online NMR system. The process of

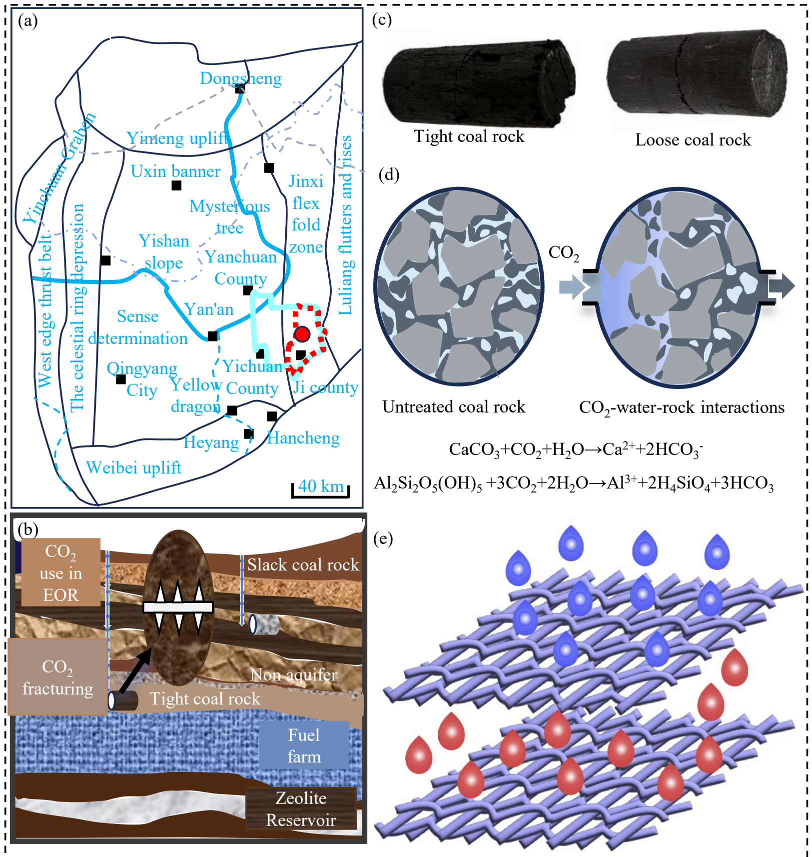

Fig. 1. Schematic diagrams of the experimental samples and techniques. (a) Structural division of the Ordos Basin, (b) schematic diagram of CO_2 injection into coal, (c) samples, (d) CO_2-water-rock interactions and (e) schematic diagram of sample imbibition in water.

dynamic NMR coal imbibition experiment is described below.

1) Core pre-treatment: the coal rock samples were dried and subsequently weighed to obtain dry mass. The T_2 spectra of the dried cores were obtained by NMR.
2) Spontaneous imbibition samples were placed in distilled water. Forced imbibition samples were placed in an intermediate vessel and the force was increased to 10 MPa after imbibition in distilled water. Carbonated water imbibition samples were placed in an intermediate container containing distilled water. Then, CO_2 gas was injected at 8 MPa, and then heated to 40 °C to reach the supercritical state. NMR analyses were performed at different imbibition times (0, 0.5, 1.5, 4.5, 16, 48 and 120 h). At the same time, the weight was accurately recorded by a high-precision balance. Fig. 2 shows the flowchart of the experimental process.

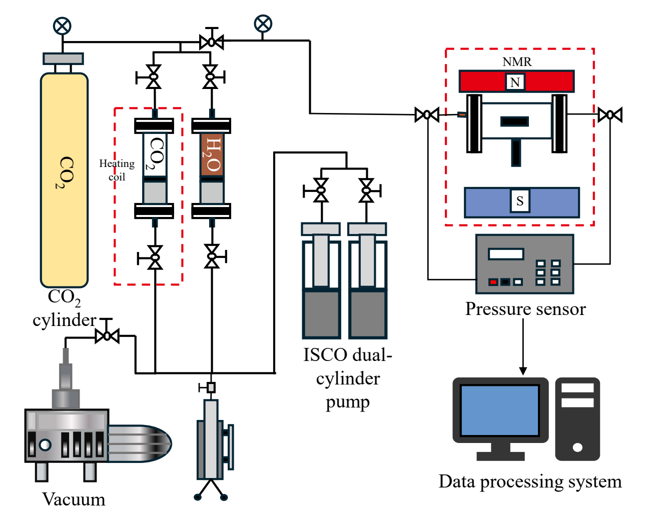

Fig. 2. Flowchart of the experimental process.

2.2.2 Mineral and pore structure characterization

(1) SEM

SEM can provide high-resolution images, which are highly suitable for observing the microscopic pore structure and dissolution effect. The resulting images can reveal the size, shape and distribution of coal pores, as well as the spread of fractures. The surface corrosion at different scales before and after SC-CO_2 immersion were analyzed based on SEM. In addition, the damage characteristics of coal rock at different scales were evaluated.

(2) NMR

The principle of NMR testing is to measure the T_2 spectrum of hydrogen-containing fluids in pores. Coal rock samples

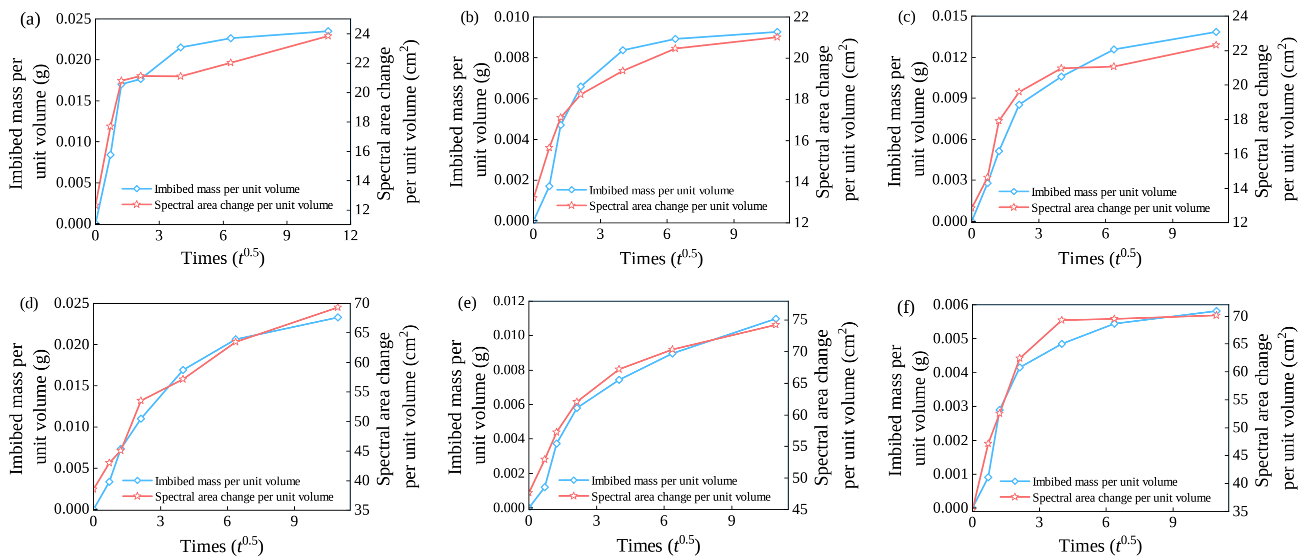

Fig. 3. Imbibed mass per unit volume and spectral area change per unit volume. (a) C1-1, (b) C1-2, (c) C1-3, (d) C2-1, (e) C2-2 and (f) C2-3.

are dried before testing. The T_2 curve can directly reflect the change of pore size and distribution, and the T_1-T_2 spectrum can reflect the occurrence state of the fluid. At the appropriate time, the samples were tested by NMR. To minimize the impact of air exposure on the experimental process, the sample was always covered in a plastic wrap during the test.

3. Results

3.1 Analysis of imbibition mass versus spectral area

In this paper, six coal samples were selected, namely three tight coal samples (C1-1, C1-2, C1-3) and three loose coal samples (C2-1, C2-2, C2-3). Imbibition experiments were carried out under three conditions: spontaneous imbibition (C1-1, C2-1), forced imbibition (C1-2, C2-2), and carbonated water imbibition (C1-3, C2-3). During the imbibition experiment, distilled water as the wetting phase was imbibed into the core interior. Since dry coal samples increase in mass after imbibition, the volume of imbibition can be calculated based on the change in mass. Dry coal matrices exhibit negligible native signals, ensuring that T_2 spectral enhancement exclusively originates from H-nuclei in distilled water, with the spectral area directly quantifying the imbibed aqueous volume. The water absorption per unit volume and spectral area variation curves are shown in Fig. 3. The curves derived from the gravimetric method and NMR T_2 spectral testing exhibit essentially consistent trends, confirming the high reliability and accuracy of experimental data.

3.2 Changes in the occurrence of pores

Prior to the experiments, cylindrical coal samples underwent 48 h of drying for the baseline hydrogen signal measurement. The tight coal samples exhibited hydrogen signals between 12-16, while the fractured samples showed signals spanning 30-45. The NMR T_2 spectra of samples at different imbibition times are shown in Fig. 4. In the spontaneous imbibition experiment, the amplitude of tight and loose coal rock samples increased rapidly in the first 1.5 h, to 18 and 47, respectively. At this time, water entered the pores of coal rocks very quickly. The increase in the mass of coal rocks verified this notion, and the mass of the C1-1 and C2-1 samples in the first 1.5 h was 1.3851 g and 4.934 g, respectively. Then, the signal of the spontaneous imbibition tight coal rock samples slowly rose to 18-19 and the signal value even decreased at 48 h. By this time, the large and medium pores in the coal rock samples had been filled with water, and only the signal value of small pores was increasing. In contrast, the signal value of the loose coal rock samples rose to 49-50, and the number of large and small pores still increased, which is related to the fact that there are more cracks in loose coal rocks.

Forced imbibition also rose rapidly in the first 1.5 h; the signal quantity of the tight coal rocks eventually rose to between 17 and 18. The signal quantity of the loose coal rock samples rose to more than 50, and the numbers of both large pores and small pores were increasing. It could be seen that forced imbibition encourages some of the pores to expand, allowing more water to enter them. In the carbonated water experiments, the small pore signal values rose in a very similar way to that in forced imbibition because the coal rocks are mainly carbonaceous and do not react with CO_2. However, the increase in the amplitude of medium and large pores was significantly stronger than that in forced imbibition. This is because CO_2 dissolves the medium and large pores of clay, allowing more water to enter.

This study classifies coal pores by relaxation time into three categories: micropores (< 1 ms), mesopores (1-10 ms), and macropores (> 10 ms). The evolution of pore signals in six experimental samples was compared, and the variation law of porosity under different permeation and absorption conditions

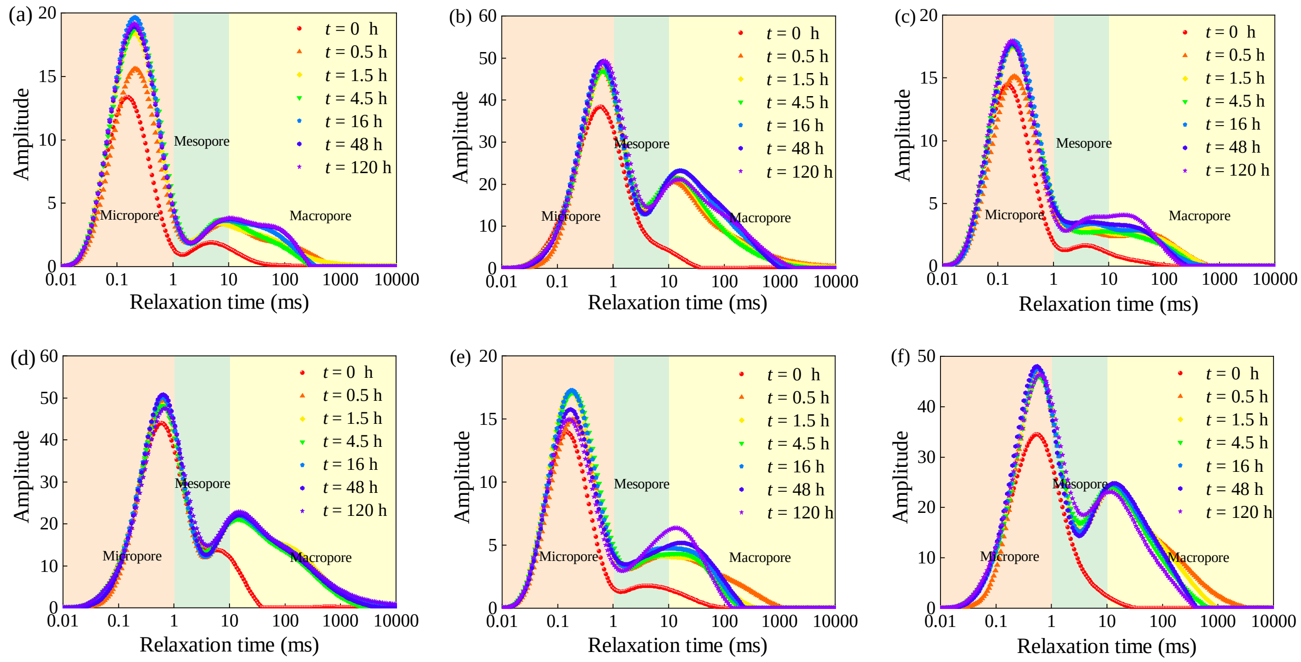

Fig. 4. T_2 spectra of samples. (a) C1-1, (b) C2-1, (c) 1-2, (d) 2-2, (e) 1-3 and (f) C2-3.

was clarified. When counting the proportion occupied by one kind of pore space, the influence caused by the increase in other pore space was ignored. The results are shown in Fig. 5. There is an overall decreasing trend in the small pore porosity of tight coal rocks, while the medium and large pore porosity shows an increasing trend. When comparing the change in porosity between tight and loose coal rocks, the small pores of loose coal rocks show a decreasing trend, while the large pore changes are obvious. There is clearly an increase in the proportion of large pores of loose coal rocks. The change in porosity after carbonated water imbibition is mainly due to the increase in the number of relatively large pores. From the experimental results shown in Fig. 5, tight coal rocks exhibit a significant decrease in micropore proportion after the reaction (15.3%), while mesopores and macropores increase by 4.4% and 11.4%. Loose coal rocks display a micropore decline of 24.8%, while mesopores and macropores increase by 2.1% and 26.9%. The comparative analysis reveals that carbonated water imbibition originates from the substantial expansion of macropores ($T_2 > 10$ ms). The macropore contribution rate increase in loose coal rocks reaches 1.7 times that of tight coal rocks.

3.3 Changes in the fluid occurrence status

Residual water primarily resides in macropores, partially in mesopores, and minimally in micropores at 0 h. After 48 h of spontaneous imbibition, sample C1-1 exhibited significant macropore expansion and increased mesopore and micropore volumes, indicating enhanced pore connectivity due to water imbibition. In loose coal samples, macropores rapidly expanded, forming fractures after imbibition. Forced imbibition further enhanced pore connectivity compared to spontaneous imbibition as a result of forced pore rupture. Carbonated water imbibition demonstrated even stronger effects, surpassing both spontaneous imbibition and forced imbibition. The changes in fluid morphology under different imbibition time are shown in Fig. 6.

Prior to the forced imbibition experiments, the loose coal rocks were significantly larger than that of the carbonated water imbibition samples. However, the area of endowed water was almost the same after the experiment. The effect of CO_2, pressure and temperature not only enlarged the large, medium and small pores originally present but also produced some new pores. The imbibition experiments indicated that the pores are dominated by large and medium sized pores in which water can easily enter, and they almost reach saturation at about 48 h of imbibition. Especially in the become larger, more numerous and more connected.

3.4 Dimensionless time

In order to perform dimensionless analysis under varying conditions, characteristic lengths are needed to handle the effects of core size and boundary conditions, which are then incorporated into calculations of dimensionless time. The shape factor F_s and characteristic length L_c can be calculated according to the following equations:

$$F_s = \frac{4}{L^2} + \frac{8}{R^2} \tag{1}$$

$$L_C = \frac{RL}{2}\sqrt{\frac{1}{R^2 + 2L^2}} \tag{2}$$

where L is length of coal rock; R is diameter of coal rock.

Since this experiment takes coal types and different imbibition conditions as variables, the idealized model assumes identical no-flow boundaries within the cores to compute the characteristic length. The L_c of tight and loose coal rocks are

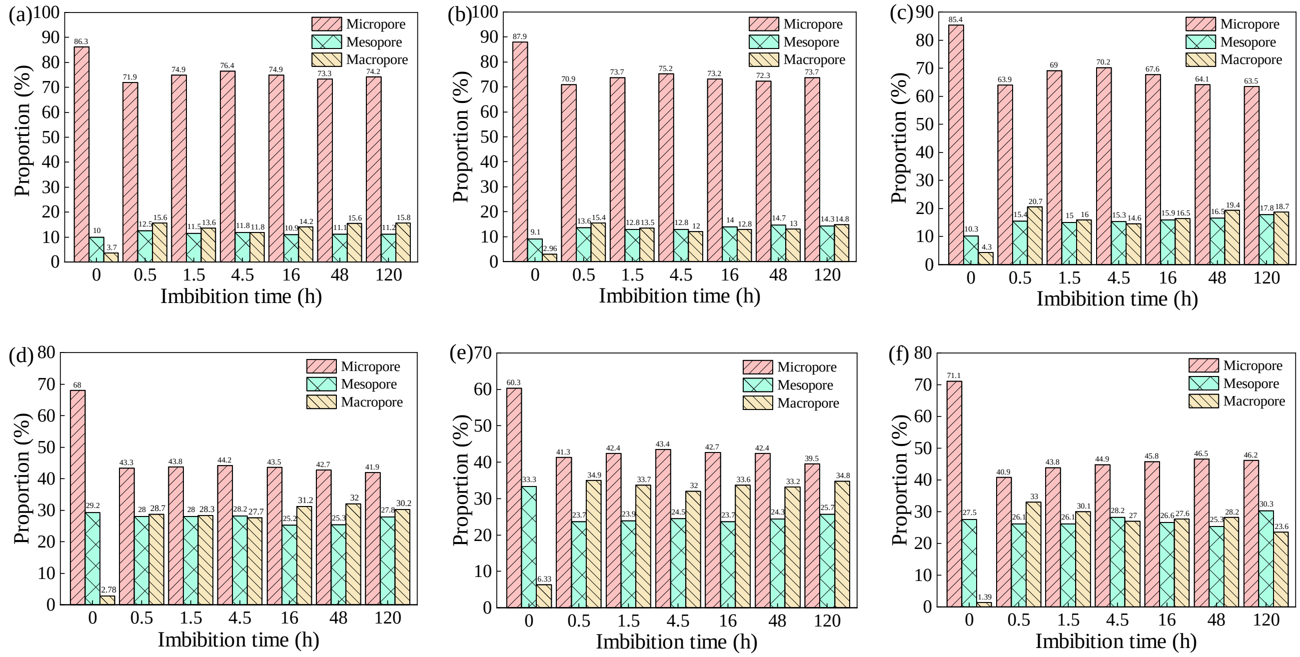

Fig. 5. Increase in the NMR T_2 spectra of core samples with different pore throat types. (a) C1-1, (b) C1-2, (c) C1-3, (d) C2-1, (e) C2-2 and (f) C2-3.

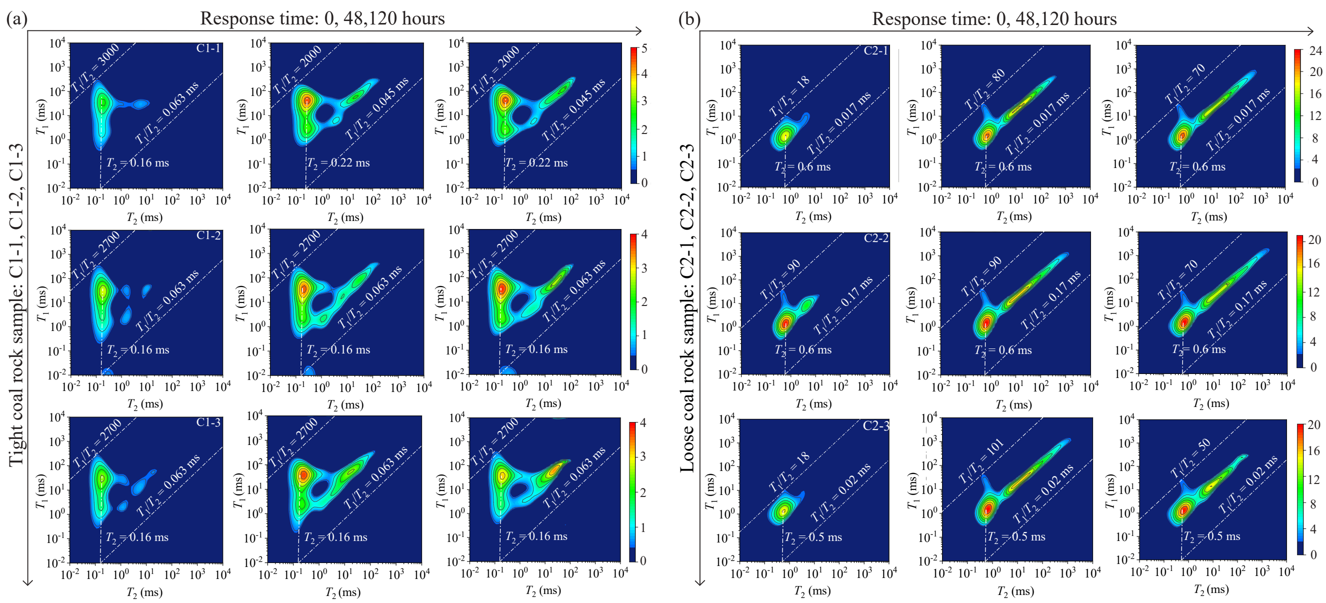

Fig. 6. Changes of fluid morphology during imbibition: (a) Tight coal rock and (b) loose coal rock.

equal, and according to Eqs. (1) and (2), L_c can be calculated as 0.4313 m.

In order to study the relationship between the imbibition time of the non-wetted phase in the core and the recovery efficiency, some scholars have proposed the concept of normalized recovery efficiency, regarding which the first recognized exponential recovery rate model is:

$$\eta = 1 - \mathrm{e}^{-\beta t} \tag{3}$$

where η is ratio of the recovery coefficient R_e to the final recovery coefficient R_∞ at time t, η is an empirical coefficient; t is imbibition time; β is power of base e.

In the no-consequence time model, the no-consequence time is directly calculated by permeability, porosity, surface tension, and other factors:

$$t_D = t\sqrt{\frac{k}{\phi}}\frac{\sigma\cos\theta}{\left(\dfrac{\mu_o}{k_{ro}} + \dfrac{\mu_w}{k_{rw}}\right)(S_{wf} - S_{wi})L_c^2} \tag{4}$$

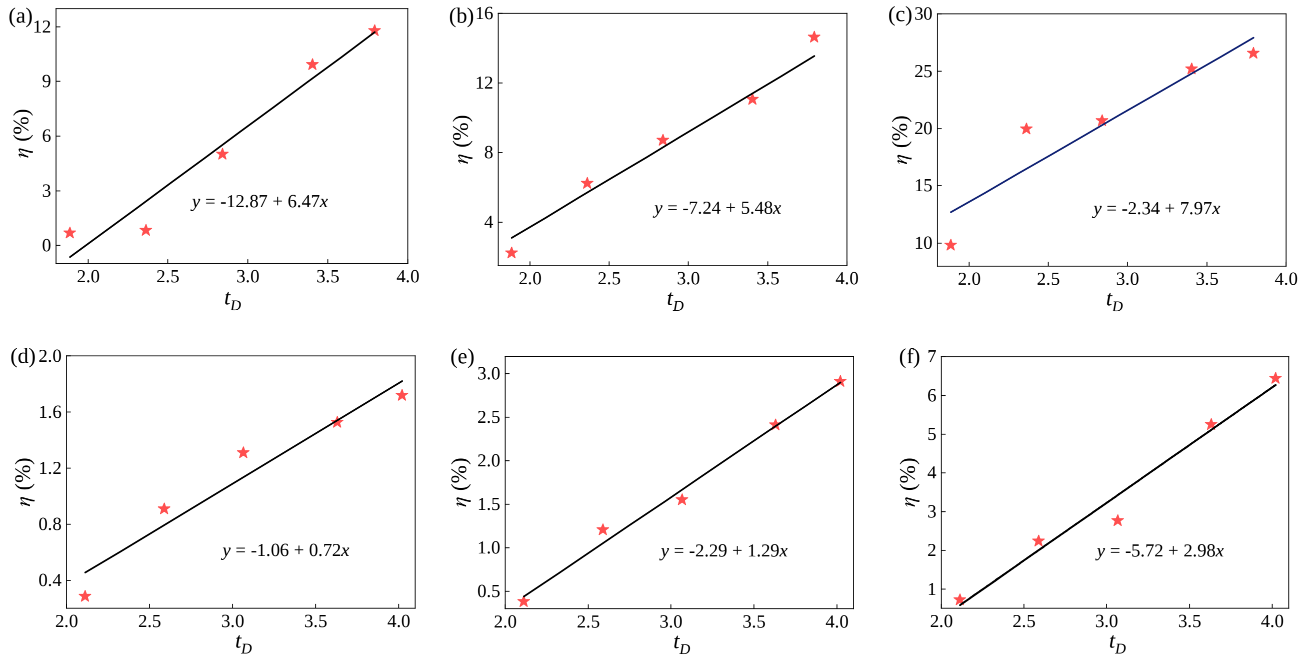

Fig. 7. Plot of t_D versus η: (a) C1-1, (b) C1-2, (c) C1-3, (d) C2-1, (e) C2-2 and (f) C2-3.

Table 1. t_D and η fit curves.

Sample	a	b
C1-1	6.47	-12.87
C1-2	5.48	-7.24
C1-3	7.97	-2.34
C2-1	0.72	-1.06
C2-2	1.29	-2.29
C2-3	2.98	-5.72

where t_D is dimensionless time; k is penetration; ϕ is porosity; μ_o is viscosity of CBM; μ_w is viscosity of distilled water; k_{ro} is relative permeability of CBM; k_{rw} is relative permeability of distilled water; S_{wf} is leading edge water saturation; S_{wi} is initial water saturation, σ is interfacial tension, θ is wetting contact angle.

Modifying the Aronofsky model and combining Eqs. (3) and (4) leads to:

$$\eta = 1 - e^{\lambda t_D} \tag{5}$$

where λ is power of base e.

The modified model, which normalizes parameters such as core dimensions and porosity, has been widely applied.

The study divides the dimensionless analysis of $\lg t_D$ and η using a breakpoint at the cutoff t_D. Thus, the following equation is formed:

$$\eta = a t_D + b \tag{6}$$

where a is slope; b is intercept.

The results are shown in Fig. 7. Since t_D increases with the progress of imbibition time, the empirical coefficient η increases with imbibition time for all three conditions. The correlation coefficients of tight coal rocks are all larger than those of loose coal rocks, and the intercept of the fitted curve is the opposite.

The relationship between the dimensionless time t_D and the empirical coefficient η in tight and loose coal rocks was analyzed using Fig. 7. According to Fig. 8, the empirical coefficient η of tight coal rocks in carbonated water imbibition is the largest, while spontaneous imbibition is the smallest. Specifically, carbonated water imbibition yields an η value 11.916% higher than forced imbibition, and forced imbibition exceeds spontaneous imbibition by 2.835%. In contrast, loose coal rocks exhibit smaller discrepancies in η among the three conditions. Carbonated water imbibition surpasses forced imbibition by 3.523%, and forced imbibition exceeds spontaneous imbibition by 1.194%.

4. Discussion

4.1 Dissolution mechanism of minerals

The results indicate that the tested coal samples contain fewer elemental species but exhibit diverse and complex intermixing patterns. Fig. 9 displays the SEM and Energy Dispersive Spectrometer scanning results of coal rock samples untreated with SC-CO_2 immersion. The samples consist of 68.7% carbon, 24.2% oxygen, and approximately equal proportions of aluminum (3.5%) and silicon (3.3%). The oxygen, aluminum and silicon elements contained fall in almost the same position, thus it was determined to be the clay mineral kaolinite. The reaction equation for kaolinite with CO_2 is given by Eq. (7), where kaolinite reacts with water and CO_2 to release aluminum ions and silicate ions. The calcite content is

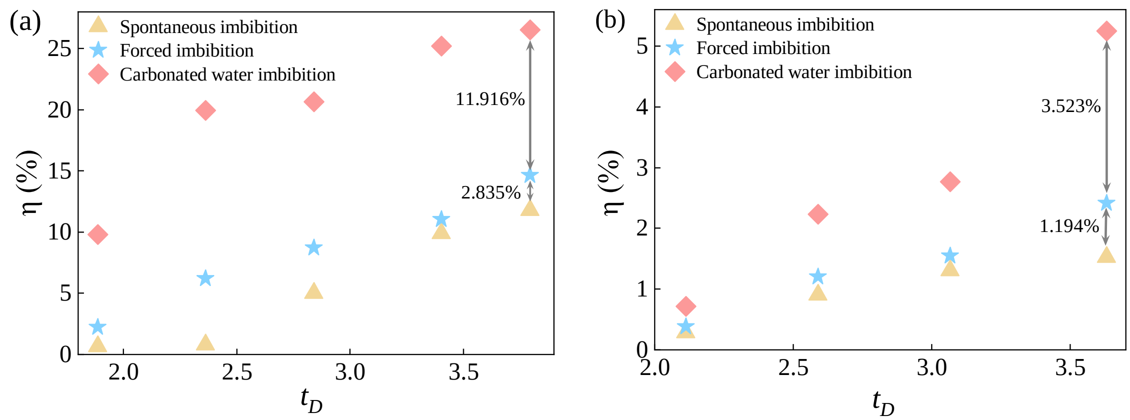

Fig. 8. Plot of t_D versus η: (a) Tight coal rock and (b) loose coal rock.

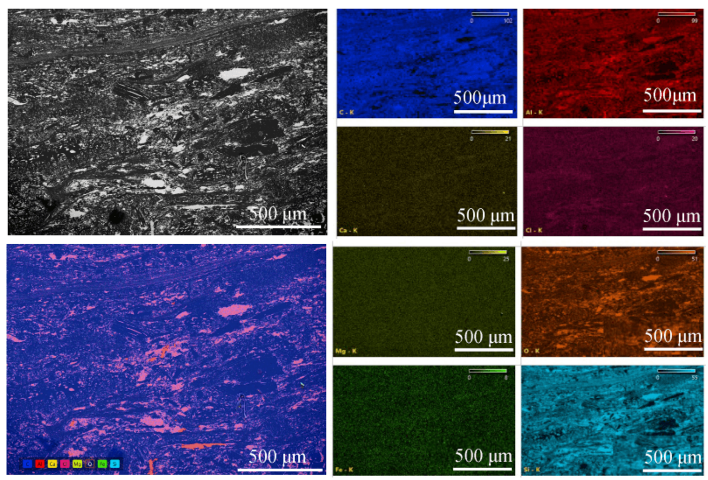

Fig. 9. Energy dispersive spectrometer results of unexposed coal rocks.

minimal, attributed to the natural defects and high brittleness of coal rocks containing calcite veinlets.

The reactions between CO_2 and minerals in coal rocks can induce mineral dissolution, precipitation, chemical transformations, and alterations in coal rock structures. When CO_2 dissolves in water to form carbonic acid, the resulting solution reacts with shale minerals as follows:

$$CO_2 + H_2O \leftrightarrow H_2CO_3 \leftrightarrow H^+ + HCO_3{}^- \tag{7}$$

$$\begin{aligned} &Al_2Si_2O_5(OH)_4 + 4CO_2 + 4H_2O \rightarrow \\ &2\,Al^{3+} + 2\,SiO_2 + 4\,HCO_3{}^- \end{aligned} \tag{8}$$

$$CaCO_3 + CO_2 + H_2O \rightarrow Ca^{2+} + 2\,HCO_3{}^- \tag{9}$$

$$\begin{aligned} &CaMg(CO_3)_2 + 2CO_2 + 2\,H_2O \rightarrow \\ &Ca^{2+} + Mg^{2+} + 4\,HCO_3{}^- \end{aligned} \tag{10}$$

$$SiO_2 + 4\,H^+ \leftrightarrow Si^{4+} + 2\,H_2O \tag{11}$$

Thus, exposure to CO_2 may alter the mechanical properties of coal rocks, especially the expansion, contraction and strength changes related to mineral reactions. Mineral dissolution can lead to increased porosity in the coal rocks, while the reprecipitation of carbonate minerals may render them harder or more tightly compacted. Carbonic acid, formed by the dissolution of CO_2, reacts with calcite in coal, resulting in its dissolution and the release of calcium ions and carbonate ions. This process is typically reversible, and calcite may reprecipitate under different pressure and temperature conditions. Similar to calcite, dolomite undergoes dissolution in CO_2-rich environments, releasing calcium and magnesium ions. Meanwhile, silicate minerals such as feldspar and mica may experience dissolution under acidic conditions. Carbonated water imbibition favors the release of metal ions from the minerals.

4.2 Mineral changes before and after SC-CO_2 treatment

For the same sample immersed in SC-CO_2, it was observed that after five days of immersion, a large fracture formed with secondary fracture. Large-sized gravel-cemented fractures exhibited complex geometries, while small-sized gravels displayed tightly bonded cementation at the millimeter scale. The large crack passing through the coal matrix at the center of the sample caused a great deal of damage, with the crack running

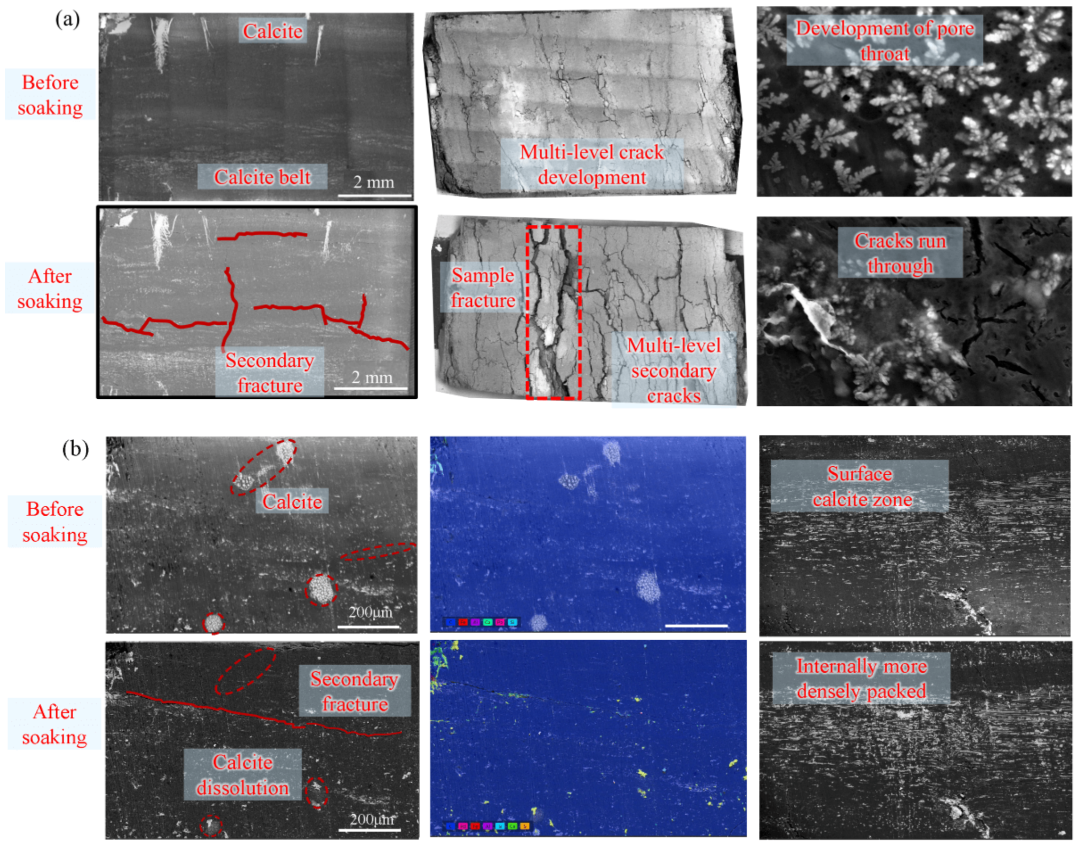

Fig. 10. Changes of fluid morphology during imbibition: (a) Tight coal rock and (b) loose coal rock.

across the entire surface of the sample. This phenomenon arises from the inherent brittleness of coal, where combined volumetric expansion and pressure development drive fracture initiation. Fig. 10 illustrates the surface damage characteristics of coal rock samples under varying immersion durations. It is worth noting that after five days of immersion, the coal rock shows obvious peeling, which might be caused by the imbibition of CO_2 into the pores. The synergistic effect of swelling caused by pore corrosion and adsorption connects the previously existing defects and microcracks.

The above processes form enlarged fractures that induce surface mineral and rock spalling. However, the concurrent marked increase in surface porosity demonstrates that CO_2 induced structural loosening at the coal rock interface. As shown in Fig. 10(b), the coal surface appears rough with abundant fractures and pores prior to immersion. However, after the calcite dissolves, the edges after immersion show peeling, dissolution pits and a smooth surface.

The microstructure and mineral distribution of the coal samples before and after acidification were analyzed at four scales using SEM. The SEM images of the coal samples were processed by computer image processing technology. For the purposes of analysis, mineral particles and organic pores were isolated from the sample matrix. In this regard, threshold segmentation is an effective image segmentation and extraction technique, where the target objects can be separated from the background by selecting appropriate thresholds.

The surface pore structure and morphology of samples before and after CO_2 immersion were analyzed via SEM. The ten-micron scale morphological changes on the coal surface are illustrated in Figs. 11(a) and 11(b). Before immersion, the coal surface shows lamellar structure and interstitial crystalline particles, whereas after immersion, intergranular pores were generated. As determined by ImageJ software processing, the surface porosity of the coal increased from 14.126% to 17.037% after CO_2 immersion. The results indicate that CO_2 reacts with the internal minerals in coal, resulting in enhanced pore development and reduced structural complexity.

Before immersion, the surface of the fifty-micron-sized coal only showed sparse interstitial particles (Figs. 11(c) and 11(d)). Meanwhile, after immersion, concretions formed, with fractures significantly propagating and multiple branched cracks and new pores emerging. After CO_2 immersion, the surface porosity of the coal increased from 14.447% to 15.219%, indicating that CO_2 interactions with the coal surface enhanced pore development. Figs. 11(e) and 11(f) illustrate the hundred-micron scale changes on the coal surface. Concretions were present in the non-immersed samples, while extensive fractures developed after immersion. Figs. 11(g) and 11(h) display the structural evolution characteristics of the coal surface at the millimeter-scale. Before immersion, the surface exhibited pronounced textural patterns, whereas after immersion, delaminated coal bodies and smoother surfaces developed. These changes increased the porosity to 11.02%, reflecting enhanced surface roughness.

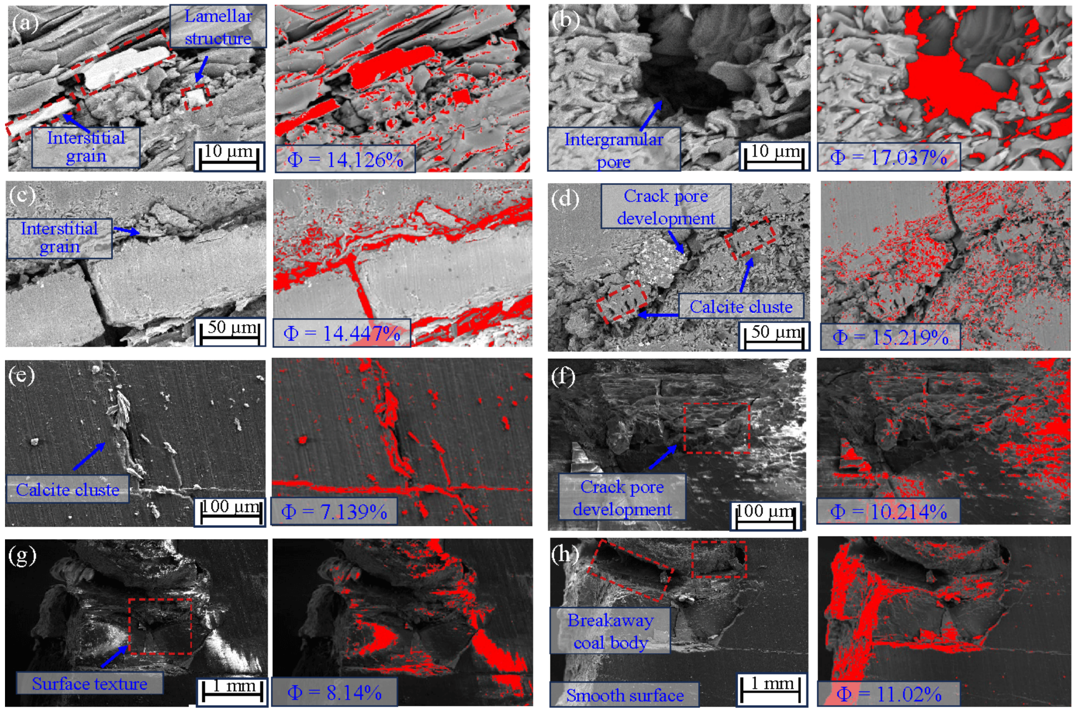

Fig. 11. SEM results of different scales of coal rock regions before and after SC-CO_2 immersion. (a)-(b) 10 μm, (c)-(d) 50 μm, (e)-(f) 100 μm and (g)-(h) 1 mm.

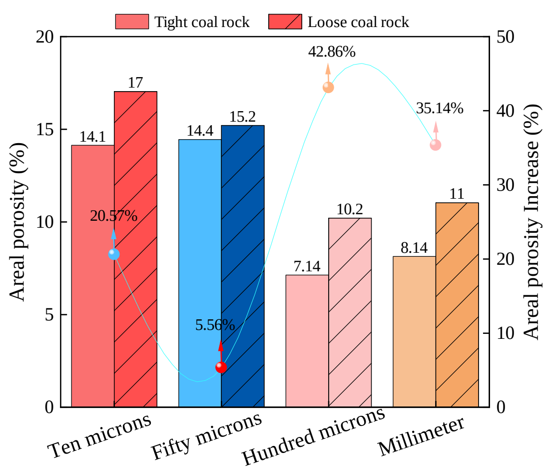

Fig. 12. Porosity at different scales in tight and loose coal rocks.

The comprehensive analysis of Fig. 12 suggests that the dissolution of minerals could lead to an increase in coal porosity. CO_2 primarily affects large pores, with a relatively low increase in porosity observed at the fifty-micron scale. At the hundred-micron scale, larger pits and complex fractures formed before and after CO_2 immersion, significantly increasing the porosity by 42.86%. At the fifty-micron scale where pores are sparse, the porosity increment after CO_2 immersion was minimal, reaching only 5.56%.

5. Conclusions

In this paper, the CO_2-water-rock interactions and microstructural damage characteristics before and after SC-CO_2 immersion were summarized for the deep eastern margin coal rocks. A series of tests were conducted to analyze the changes in mineral composition and fluid occurrence before and after SC-CO_2 immersion. The conclusions of comprehensive analysis are as follows:

1) In the process of CO_2-water-rock interaction, the pore structure will expand due to dissolution, and the secondary precipitation of minerals will block part of the pore space. The results of NMR T_2 show that the amplitude of the four cores increases by 27.7%, 8%, 34.7%, and 37.5% after CO_2 immersion, respectively, and the occurrence frequency of carbonated water in the cores increases. It is found that the change of porosity after carbonated water saturation is mainly due to pore expansion, resulting in an increase in the number of relatively large pores. NMR T_1-T_2 spectra reveal that the concentration and range of carbonated water rises, and the content of movable water in large pores changes significantly.
2) A dimensionless framework for analyzing imbibition in both tight and loose coal was established by introducing a characteristic length to normalize core dimensions and boundary conditions. Tight coal rocks exhibit higher fitting coefficients, while smaller inter-sample differences are observed for loose coal rocks. These results demonstrate the critical role of coal anisotropy in imbibition efficiency under varying physicochemical conditions.
3) After immersion in SC-CO_2, significant damage occurred on the surface of the coal rocks, manifested as the generation and expansion of cracks. In addition, with the progress of imbibition time, the size and number of

cracks gradually increase, the surface of the coal rock becomes looser, and the pore development becomes more complex. The expansion induced by SC-CO_2, especially in the brittleness of coal rock, leads to the occurrence of cracks and surface spalling. This process is closely related to the dissolution of minerals, especially that of calcite, which intensifies the increase in the surface porosity of coal rock.

4) After SC-CO_2 immersion, obvious cracks appear on the surface of the coal rock, which continue to expand during handling, resulting in the reduced integrity of the coal rock. At the same time, some clay minerals gradually dissolve under the action of SC-CO_2 and lose their original structural stability. Furthermore, some coal rocks adsorbed SC-CO_2, causing expansion and eventually shedding, further altering the physical properties and surface characteristics of the coal rock.

Acknowledgements

This work was supported by the National Natural Science Foundation of China (No. 52374014) and the Fundamental Research Funds for the Central Universities (No. 2024ZKPYSB03).

Conflict of interest

The authors declare no competing interest.

References

Bakhshian, S., Sahimi, M. Adsorption-induced swelling of porous media. International Journal of Greenhouse Gas Control, 2017, 57: 1-13.

Cai, J. Some key issues and thoughts on spontaneous imbibition in porous media. Chinese Journal of Computational Physics, 2021, 38(5): 505-512. (in Chinese)

Cai, J., Perfect, E., Cheng, C., et al. Generalized modeling of spontaneous imbibition based on Hagen-Poiseuille flow tortuous capillaries with variably shaped apertures. Langmuir, 2014, 30(18): 5142-5151.

Chen, K., Liu, X., Wang, L., et al. Influence of sequestered supercritical CO_2 treatment on the pore size distribution of coal across the rank range. Fuel, 2021, 306: 121708.

Fang, H., Li, A., Sang, S., et al. Numerical analysis of permeability rebound and recovery evolution with THM multi-physical field models during CBM extraction in crushed soft coal with low permeability and its indicative significance to CO_2 geological sequestration. Energy, 2023, 262: 125395.

Hou, J., Hu, X., Zhao, Y., et al. Z. Improvement of wettability of coal seams in water injection via co-deposition of polydopamine and polyacrylamide. Colloids and Surfaces A: Physicochemical and Engineering Aspects, 2022, 636: 128112.

Huang, R., Jiang, Z., Gao, Z., et al. Influence of shale reservoir fabric characteristics on spontaneous infiltration. Oil-gas Geology and Recovery, 2017, 24(1): 111-115. (in Chinese)

Huang, Z., Xing, H., Zhou, X., et al. Numerical study of vug effects on acid-rock reactive flow in carbonate reservoirs. Advances in Geo-Energy Research, 2020, 4(4): 448-459.

Jiao, X., He, W., Tian, Z., et al. Characterization of water micro-distribution behavior in shale nanopores: A comparison between experiment and theoretical model. Advances in Geo-Energy Research, 2025, 15(1): 79-86.

Liao, Z, Liu, X., Song, D., et al. Micro-structural damage to coal induced by liquid CO_2 phase change fracturing. Natural Resources Research, 2021, 30(2): 1613-1627.

Li, C., Tan, M., Wang, Z., et al. Nuclear magnetic resonance pore radius transformation method and fluid mobility characterization of shale oil reservoirs. Geoenergy Science and Engineering, 2023, 221: 211403.

Li, C., Yang, D., Xie, H., et al. Research on the anisotropic fracture behavior and the corresponding fracture surface roughness of shale. Engineering Fracture Mechanics, 2021, 255: 107963.

Li, J., Huang, Q., Wang, G., et al. Experimental study of effect of slickwater fracturing on coal pore structure and methane adsorption. Energy, 2022a, 239: 122421.

Li, K., Kong, S., Xia, P., et al. Microstructural characterization of organic matter pores in coal-measure shale. Advances in Geo-Energy Research, 2020, 4(4): 372-391.

Liu, X., Nie, B., Guo, K., et al. Permeability enhancement and porosity change of coal by liquid carbon dioxide phase change fracturing. Engineering Geology, 2021, 287: 106106.

Liu, X., Wang, L., Kong, X., et al. Role of pore irregularity in methane desorption capacity of coking coal. Fuel, 2022, 314: 123037.

Li, X., Zhang, Q., Liu, P., et al. Investigation on the microscopic damage mechanism of fracturing fluids to low-permeability sandstone oil reservoir by nuclear magnetic resonance. Journal of Petroleum Science and Engineering, 2022b, 209: 109821.

Lu, Y., Liu, D., Cai, Y., et al. Spontaneous imbibition in coal with *in-situ* dynamic micro-CT imaging. Journal of Petroleum Science and Engineering, 2022, 208: 109296.

Ma, Y., Deng, Z., Yue, J., et al. Nuclear magnetic resonance experiment on the influence of confining pressure on spontaneous imbibition of water in coal. Energy & Fuels, 2022, 36: 4818-4829.

Nguyen, P., William, C., Hari, S., et al. Effectiveness of supercritical-CO_2 and N_2 huff-and-puff methods of enhanced oil recovery in shale fracture networks using microfluidic experiments. Applied Energy, 2018, 230: 160-174.

Niu, Q., Cao, L., Sang, S., et al. Experimental study on the softening effect and mechanism of anthracite with CO_2 injection. International Journal of Rock Mechanics and Mining Sciences, 2021, 138: 104614.

Si, L., Zhang, H., Wei, J., et al. Modeling and experiment for effective diffusion coefficient of gas in water-saturated coal. Fuel, 2021, 284: 118887.

Wang, J., Liu, H., Xia, J., et al. Mechanism simulation of oil displacement by imbibition in fractured reservoirs. Petroleum Exploration and Development, 2017, 44(5): 805-814.

Wei, J., Shang, D., Zhao, X., et al. Experimental study on production characteristics and enhanced oil recovery during imbibition and huff-n-puff injection in shale reservoir. Capillarity, 2024, 12(2): 41-56.

Wei, J., Wang, A., Wang, R., et al. Contribution of different shale storage spaces to recovery rate and mechanism of oil mobilization during imbibition. Capillarity, 2025, 15(1): 12-24.

Wei, M., Liu, J., Elsworth, D., et al. Influence of gas adsorption induced non-uniform deformation on the evolution of coal permeability. International Journal of Rock Mechanics and Mining Sciences, 2019, 114: 71-78.

Xia, Y., Tian, Z., Xu, S., et al. Effects of microstructural and petrophysical properties on spontaneous imbibition in tight sandstone reservoirs. Journal of Natural Gas Science and Engineering, 2021, 96: 104225.

Xu, C., Xu, H., Zhang, L., et al. Spatial functional division, infrastructure and carbon emissions: Evidence from China. Energy, 2022, 256: 124551.

Yang, L., Jiang, X., Li, M. et al. Pore-scale numerical simulation of spontaneous imbibition in porous media containing fractures. Capillarity, 2024, 10(2): 48-56.

Yang, L., Liu, Y., Wang, W., et al. Pore-scale flow mechanism of immiscible gas-assisted gravity drainage in strongly heterogeneous glutenite reservoirs. International Journal of Coal Science & Technology. 2025a, 12: 12.

Yang, L., Zhao, Z., Zhang, J., et al. Spontaneous imbibition laws of fracture-containing porous media based on phase field theory. Petroleum Science Bulletin, 2025b, 10(2): 269-282. (in Chinese)

Yuan, L. Control of coal and gas outbursts in Huainan mines in China: A review. Journal of Rock Mechanics and Geotechnical Engineering, 2016, 8(4): 559-567.

Yue, J., Wang, Z., Fan, Y., et al. Feasibility study of testing imbibition effect in coal containing gas with isobaric pressure relief device. Journal of Safety Science and Technology, 2017, 13(10): 110-114. (in Chinese)

Zhang, S., Liu, J., Wei, M., et al. Coal permeability maps under the influence of multiple coupled processes. International Journal of Coal Geology, 2018, 187: 71-82.

Zhang, S., Yan, J., Hu, Q., et al. Integrated NMR and FE-SEM methods for pore structure characterization of Shahejie shale from the Dongying Depression, Bohai Bay Basin. Marine and Petroleum Geology, 2019, 100: 85-94.